Interphases, gelation, vitrification, porous glasses and the generalized Cauchy relation: epoxy/silica nanocomposites

2009 New J. Phys. 11 023015

(http://iopscience.iop.org/1367-2630/11/2/023015)

New Journal of Physics
The open-access journal for physics

Interphases, gelation, vitrification, porous glasses and the generalized Cauchy relation: epoxy/silica nanocomposites

M Philipp[1,4], U Müller[1], R J Jiménez Riobóo[1,2,5], J Baller[1], R Sanctuary[1], W Possart[3] and J K Krüger[1]

[1] Laboratoire de Physique des Matériaux, University of Luxembourg, 162A avenue de la Faïencerie, L-1511 Luxembourg, Luxembourg
[2] Instituto de Ciencia de Materiales de Madrid (CSIC), Campus de Cantoblanco s/n, E-28049 Madrid, Spain
[3] Fachbereich Werkstoffwissenschaften, Universität des Saarlandes, D-66123 Saarbrücken, Germany
E-mail: martine.philipp@uni.lu

New Journal of Physics **11** (2009) 023015 (13pp)
Received 29 October 2008
Published 9 February 2009
Online at http://www.njp.org/
doi:10.1088/1367-2630/11/2/023015

Abstract. The generalized Cauchy relation (gCR) of epoxy/silica nanocomposites does not show either the chemically induced sol–gel transition or the chemically induced glass transition in the course of polymerization. Astonishingly, by varying the silica nanoparticles' concentration between 0 and 25 vol% in the composites, the Cauchy parameter A of the gCR remains universal and can be determined from the pure epoxy's elastic moduli. Air-filled porous silica glasses are considered as models for percolated silica particles. A longitudinal modulus versus density representation evidences the aforementioned transition phenomena during polymerization of the epoxy/silica nanocomposites. The existence of optically and mechanically relevant interphases is discussed.

[4] Author to whom any correspondence should be addressed.
[5] Guest Scientist at the Laboratoire de Physique des matériaux, University of Luxembourg, 162A avenue de la Faïencerie, L-1511 Luxembourg, Luxembourg.

Contents

1. Introduction

The linear elastic properties of isotropic materials like amorphous solids and nanocrystalline ceramics are usually believed to be fully characterized by two independent elastic moduli, e.g. the longitudinal modulus c_{11} and the shear modulus c_{44} [1]–[5]. This also holds true for the high-frequency clamped longitudinal and shear moduli c_{11}^{∞} and c_{44}^{∞} of isotropic liquids (i.e. when measured at sufficiently high frequencies) [1, 2, 4], whereas the static shear modulus of liquids is zero. Only recently has it been shown that the so-called generalized Cauchy relation (gCR)

$$c_{11}^{\infty}\left(c_{44}^{\infty}\right) = 3 \cdot c_{44}^{\infty} + A \tag{1}$$

is applicable to elastic moduli following Hooke's law for various isotropic materials such as structural glass formers, polymers, nanoceramics, and metallic glasses [6]–[14]. The constant quantity A in equation (1), in the following called the 'Cauchy parameter', is a characteristic parameter for a given material [6]–[14]. The gCR yields a linear relationship between the longitudinal and shear moduli of a given isotropic material assuming that c_{44}^{∞} is an independent variable. It is supposed that c_{44}^{∞} can be varied by external parameters like temperature T, pressure p, chemical conversion, etc. The important message of equation (1) is that the number of independent elastic moduli is reduced to one, once the Cauchy parameter A is known. Different parameters capable of driving the elastic moduli according to gCRs have been reported in the literature: (i) temperature [7]–[14], (ii) chemical conversion [6, 7, 9, 13, 14], (iii) mixing ratio of the epoxy's constituents [7, 9, 13] and even (iv) different amounts of nanoparticles in a liquid matrix [9]. Non-equilibrium effects like polymerization or vitrification are tolerated by the gCR if the elastic moduli reach their local equilibrium during the collection time of each data point [7, 8, 14]. In addition, the gCR has been evaluated for combinations of driving parameters: for instance, temperature-dependent measurements of c_{11}^{∞} and c_{44}^{∞} have been performed on the same type of oligomer filled with different amounts of nanoparticles [9], yielding the same Cauchy parameter A independently of the temperature and concentration of nanoparticles. Another example is the identical gCRs observed during the polymerization of polyurethanes and during temperature changes performed after having cured the polyurethanes [14]. In the present work, we are interested in the alternative combination of driving parameters 'chemical conversion' and 'concentration of nanoparticles'. Especially this combination is of physical as well as technical importance. The system in which we are interested is a commercially available epoxy/silica nanocomposite.

The phenomenological properties of nanocomposites usually depend strongly in a nonlinear manner on the concentration of nanoparticles within the matrix [15]. If nanoparticles are incorporated into a matrix it is believed that at the boundary between the nanoparticles and the surrounding matrix, the so-called interphases are built up [15]–[17]. These interphases are part of the matrix but their morphology is assumed to differ from that of the bulk. The morphology of the interphases might have physical and/or chemical origin. In addition, the dimensions of these interphases might appear different for different physical quantities.

In this paper we will focus on

(1) the superimposing and possibly competing effects of the epoxy's polymerization and the interactions between the epoxy's constituents and the nanoparticles at the epoxy/silica boundary including the formation of interphases. In the framework of the gCR, the elastic properties of the pure epoxy, epoxy/silica nanocomposites, porous silica glasses and fused silica will be compared;
(2) porous silica glasses as model systems for percolated silica nanoparticles as a function of porosity (or density); and
(3) the role of isostructural transitions such as the chemically induced sol–gel and glass transitions [18]–[21] during polymerization.

All measurements are performed with high-performance Brillouin spectroscopy (BS) or high-precision refractometry.

2. Experimental

2.1. Samples and sample preparation

Since we investigate the mechanical and optical properties of nanocomposites by optical methods (i.e. BS and refractometry), we chose commercial products that possess an outstanding transparency:

(1) a diglycidyl ether of bisphenol A (DGEBA) resin filled with silica nanoparticles in the mass ratio DGEBA/silica (100 : 67) (Nanopox A410; Nanoresins AG, Germany). The silica particles have an average diameter of 20 nm and are produced by a sol–gel process inside the matrix. They are amorphous with questionable density and possess a silane coating at their surfaces. Considering the assumptions made in order to calculate the density and the refractive indices of the silica particles, the differences between the properties of the silica particles and those of fused silica, indicated in table 1, are not relevant;
(2) the pure DGEBA resin as present in Nanopox A410, possessing an epoxy equivalent weight of roughly 177 g/eq. It was used to dilute the Nanopox resin; and
(3) diethylene triamine (DETA) with purity above 97% as the hardener (Fluka Chemie, Switzerland).

The mechanical properties of these commercially available nanocomposites have mostly been studied in the linear and nonlinear response regime including yield behavior [16], [23]–[29]. Great efforts have been made to provide relationships between the desired mechanical properties and the morphology of the nanocomposites [23]–[27]. Among others, scanning electron microscopy, transmission electron microscopy and atomic force microscopy

Table 1. Properties of the nanocomposites' constituents at 298 K.

Sample	Density ρ (g cm^{-3})	Refractive index n_D	c_{11} (GPa)	c_{44} (GPa)
DETA	0.95 ± 0.01[a]	1.482 ± 10^{-3}	3.3 ± 0.1[d]	
Pure DGEBA	1.16 ± 0.01[a]	1.571 ± 10^{-3}	7.0 ± 0.1[d]	1.5 ± 0.5[d]
Nanopox A410	1.4 ± 0.1[a]	1.545 ± 10^{-3}	9.8 ± 0.1[d]	2.4 ± 0.5[d]
Silica particles	2.0 ± 0.2[b]	1.48 ± 0.02[b]		
Fused silica [22]	2.20 ± 0.01	1.463 ± 10^{-3}[c]	76 ± 1	31 ± 1

[a] Product data sheet.
[b] Estimated density and refractive index using those of Nanopox A410 and pure DGEBA (linear mixing rules). The term 'silica particle' should be understood as the pure silica core and its silane shell.
[c] Determined at 300 K and 514 nm.
[d] Determined at 295 K and GHz frequencies.

have been used as investigation techniques for elucidating the local structure of these composites including interphases [27]. The average mean diameter of the silica nanoparticles given by the producer was confirmed by electron microscopic investigations of Kinloch and coworkers and Rosso and Ye [23]–[27].

For our investigations, first three silica-filled DGEBA samples were prepared at ambient temperature (DGEBA/silica mass ratio: (100 : 67), (100 : 25) and (100 : 11)). In order to start the polymerization, the hardener DETA was added to the resins in the mass ratio of pure DGEBA/DETA of (100 : 14.2). A pure epoxy without any nanoparticles (i.e. DGEBA/DETA/silica (100 : 14.2 : 0)) was studied as a reference. The total sample masses were always below 3 g in order to avoid self-heating effects. The samples were mixed for 1 min at 3000 rpm by using a Speedmixer^{TM} (Hauschild, Germany). These epoxies are slightly over-stoichiometric (stoichiometric: DGEBA/DETA (100 : 12)). The pure epoxy (100 : 14.2) shows the highest tensile shear strength during fracture experiments performed on different epoxy mixtures glued on native aluminium [16, 28]. The polymerizations were studied at 298 K when the chemical sol–gel and/or glass transition take place for all nanoparticle concentrations [16, 28, 29]. According to the model of Bansal and Ardell [30], the mean interparticle distance (surface–surface distance) between the silica nanoparticles can be estimated to be below 25 nm for all nanocomposites (see table 3).

The porous silica glasses were purchased from the companies Geltech and Corning. The four Geltech glasses called Gelsil (see table 2) were produced by a sol–gel process. At the origin of the investigated Vycor glass from Corning was the spinodal decomposition of a boro-silica glass. The boria phase was eliminated under acid attack. All the investigated glasses were optically transparent and possessed silica purity above 96%; further properties are given in table 2.

2.2. Brillouin spectroscopy (BS)

As we are interested in the evolution of the high-frequency clamped longitudinal and shear moduli, c_{11}^{∞} and c_{44}^{∞}, at the crossover from the liquid to the solid isotropic state of epoxy/silica nanocomposites, high performance BS was used. The epoxy/silica nanocomposites were of

Table 2. The properties of the porous silica glasses at room temperature.

Silica glass	Pore diameter (nm) [a]	Porosity (%) [a]	Density ($g\,cm^{-3}$) [a]	c_{11}(GPa) [b]	c_{44}(GPa) [b]
Vycor 7930	4	30	1.5	15.5	5.92
Gelsil 025	2.5	48	1.2	12.8	4.75
Gelsil 050	5	63	0.9	6.94	2.60
Gelsil 075	7.5	70	0.7	1.39	0.52
Gelsil 200	20	78	0.6	1.34	0.53

[a]Product data sheet.
[b]Determined at GHz frequencies by using BS.

good optical transparency which is a prerequisite for reliable Brillouin spectroscopic results. This optical transparency is in accordance with the average particle diameter of 20 nm and the absence of silica particle agglomerates [23]–[27]. The samples were filled into self-built 1 mm thick aluminium-ring cuvettes with two glass windows and placed inside a self-made helium-flooded optical thermostat, which was temperature stabilized at 298 K. While investigating chemical reactions, the accumulation time for the Brillouin spectra has to be short (≈5 min) as compared with the progress of the chemical reaction. Further details of the measurement technique are given in [21, 31]. The longitudinal and transverse sound frequencies $f_{\mathrm{L,T}}$ were determined simultaneously in the 90A scattering geometry, where the acoustic wavelength Λ^{90A} is strictly independent of the refractive index [21, 31]. By measuring the sound frequencies $f_{\mathrm{L,T}}\left(\vec{q}^{\,90A}\right)$, the longitudinal and transverse sound velocities v_L^∞ and v_T^∞ can be calculated:

$$v_{\mathrm{L,T}}^{\infty} = f_{\mathrm{L,T}}\left(\vec{q}^{\,90A}\right) \cdot \Lambda^{90A} = f_{\mathrm{L,T}}\left(\vec{q}^{\,90A}\right) \cdot \frac{\lambda_{\mathrm{LASER}}}{\sqrt{2}}, \tag{2}$$

where λ_{LASER} is the vacuum laser wavelength and $\Lambda^{90A} = 376$ nm is the acoustic wavelength related to the 90A scattering geometry and $\left|\left(\vec{q}^{\,90A}\right)\right| = 2\pi/\Lambda^{90A}$ is the related phonon wave vector [21, 31].

As BS was performed on thermal phonons, the sound frequencies were measured in linear response. Thus, with a knowledge of the mass density ρ of the sample, the longitudinal and shear moduli c_{11}^∞ and c_{44}^∞ can be determined by using

$$c_{11,\,44}^{\infty} = \rho \cdot (v_{\mathrm{L,\,T}}^{\infty})^2. \tag{3}$$

2.3. Refractometry

The refractive indices n of the nanocomposites were measured during the polymerizations at 298 K with a high-precision refractometer (Abbemat; Anton Paar OptoTec GmbH, Germany) for the optical wavelength 589.3 nm. This refractometer has the high absolute accuracy of 10^{-5} and a relative accuracy of 10^{-6}. The measurement chamber was specially sealed against moisture during the investigations. After the experiments, the glassy adhesives could be removed from the YAG prism after a suitable chemical treatment. As for BS, good optical

transparency of the samples is essential. Using the measured refractive indices, the mass densities ρ were determined by the Lorentz–Lorenz relation [32, 33]:

$$\rho = \frac{1}{r} \cdot \frac{n^2 - 1}{n^2 + 2}, \tag{4}$$

where r is the specific refractivity. It was shown for epoxies that the specific refractivity is almost constant during polymerization at ambient temperature [28].

3. Theoretical background of Cauchy relations (CRs)

CRs are originally a topic of solid state physics concerning the linear elastic behavior of crystals [1]–[4]. They reduce the number of independent components of the elastic tensor for a given symmetry if the following prerequisites are fulfilled: (i) no lattice anharmonicity, (ii) every lattice point is a centre of inversion, and (iii) only central forces act between lattice sites. CRs usually do not apply in a dynamic elastic regime where the elastic moduli become complex quantities. The problem of related acoustic excess attenuation can often be overcome by using hypersonic frequencies as measured by BS.

As was already reported by Sommerfeld [3], CRs are not expected to hold for isotropic, for instance amorphous materials. In the 1960s, Zwanzig and Mountain [34] calculated a kind of generalized CR for the high-frequency clamped elastic moduli of simple liquids:

$$c_{11}^{\infty} = 3 \cdot c_{44}^{\infty} + A(T, p, \ldots). \tag{5}$$

According to these authors, the parameter $A = A(T, p, \ldots)$ depends on external driving parameters such as temperature T, and pressure p. In accordance with the remark of Sommerfeld, equation (5) does not reduce the number of independent elastic moduli from two to one.

As mentioned in the introduction, only recently gCRs with a constant parameter A according to equation (1) have been observed for many glasses, liquids and ceramics [6]–[14]. In the following, the term gCR will be used only in this sense.

We want to stress that, at the beginning of the chemical reaction, our epoxy/silica nanocomposites behave as liquids when measured at low probe frequencies. On increasing the probe frequency, e.g. toward the GHz regime, the elastic properties undergo, in the regime of acoustic excess attenuation, a transition from the so-called 'fast motion regime' to the 'slow motion regime' [2, 21, 31]. In the slow motion regime, even liquids follow Hooke's law [1]–[5], yielding the two high-frequency clamped elastic moduli c_{11}^{∞} and c_{44}^{∞}.

4. Results and discussion

The temporal evolution of the longitudinal and transverse hypersonic velocities v_L and v_T as well as that of the hypersonic attenuations Γ_L and Γ_T are given in figures 1 and 2 for the polymerization of the pure epoxy and the three epoxy/silica nanocomposites described in section 2.1. The longitudinal and transverse sound velocities show qualitatively the same behavior for all samples: both quantities increase in the course of polymerization and tend to saturate after about 6 h. An increasing amount of silica leads to higher sound velocities (i.e. elastic moduli) of the nanocomposites, indicating that the silica particles possess higher moduli than the epoxy. As usual, the optoacoustic coupling coefficient (Pockels coefficient [2])

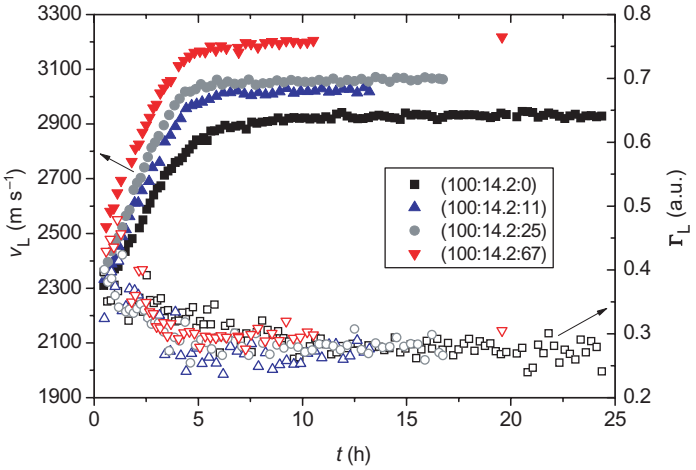

Figure 1. Longitudinal hypersonic velocities v_L (filled symbols) and hypersonic attenuations Γ_L (open symbols) versus time during the polymerization of the epoxy (100 : 14.2 : 0) and the three epoxy/silica nanocomposites.

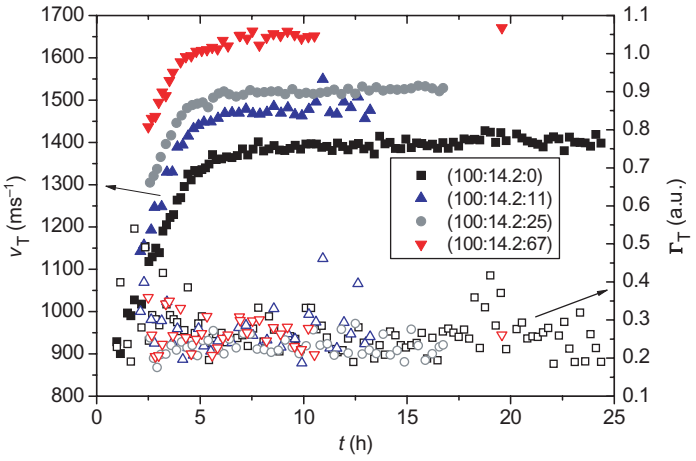

Figure 2. Transverse hypersonic velocities v_T (filled symbols) and hypersonic attenuations Γ_T (open symbols) versus time during the polymerization of the epoxy (100 : 14.2 : 0) and the three epoxy/silica nanocomposites.

is greater for the longitudinal than for the transverse mode, which results in a smaller Brillouin scattering intensity of the transverse mode and therefore in a slightly greater data scatter. Due to the small Pockels coefficients of silica compared with those of epoxy, the transverse phonons of the nanocomposites are more and more difficult to record with increasing silica concentration.

According to the small average nanoparticle diameter of about 20 nm and the lack of silica particle agglomerates [23]–[27], the nanocomposites lead only to optic and acoustic Rayleigh scattering, but fortunately neither to optical nor to acoustic Mie scattering [35, 36], which would be much stronger if present. Correspondingly, the acoustic damping of the phonons given in figures 1 and 2 is not increased significantly by the nanoparticles. Thus, our nanocomposites can be described perfectly by continuum mechanics in linear response. As the hypersonic excess

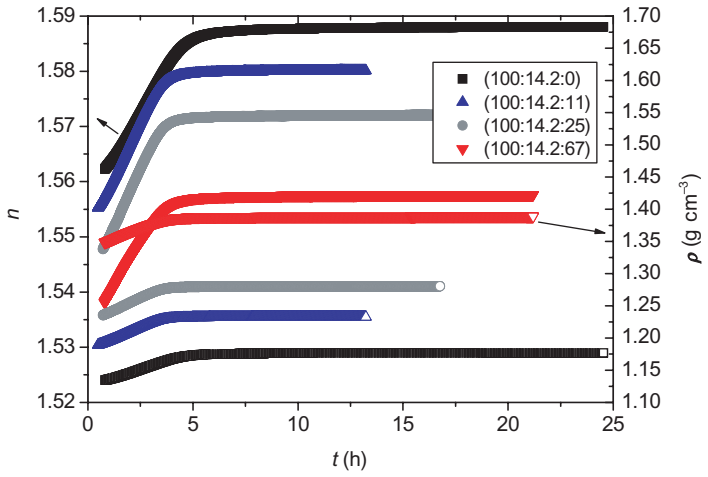

Figure 3. Refractive indices n (filled symbols) and densities ρ (open symbols) versus time during the polymerization of the epoxy (100 : 14.2 : 0) and the three epoxy/silica nanocomposites. The densities were calculated from the refractive index data using the Lorentz–Lorenz relation [32, 33].

attenuation is only present during the first three hours of polymerization, this attenuation is due to molecular relaxations. All sound velocity data measured after 3 h can be treated as high-frequency clamped quantities.

As shown in figure 3, increasing the amount of silica nanoparticles within the nanocomposites causes a systematic decrease in the absolute values of the refractive indices. Applying a simple mixing rule to the refractive indices of DGEBA, DETA and the silica particles (see table 1), these calculated values agree well with the data extrapolated from the measured ones to the beginning of the experiment (relative error $< 1\%$).

During the first six hours of polymerization, all refractive indices show an important increase before saturating. As expected, the relative refractive index increase is the highest for the pure epoxy sample during polymerization (see table 3). For this calculation only refractive indices measured after 0.8 h were used in order to eliminate initial influences of sample preparation (e.g. air bubbles). Optical interphases, in the sense of modified optical properties in the vicinity of the nanoparticles in the epoxy, could not be detected: no significant differences between the nanocomposites' refractive indices and those obtained by applying a simple mixing rule to the pure epoxy's and the particles' refractive indices could be obtained between 0.8 and 13 h.

Neither the hypersonic properties nor the related refractive indices give a specific hint for the chemically induced sol–gel or glass transitions, which occur in all samples in the course of polymerization [16, 28, 29]. It is worth noting that the strong bending of the sound velocity and the refractive index curves is linked to the saturation of the polymerization, which can result either from the consumption of all reactive groups or from a chemically induced glass transition. Thus, this strong bending is not *a priori* indicative of any phase transition.

In order to calculate the time evolution of the densities (see figure 3, open symbols), the specific refractivities r of the samples had to be determined (see equation (4)). The densities of the samples at the beginning of the chemical reaction were estimated by assuming the volume additivity of DGEBA, DETA and silica particles. Combining these densities with the

Table 3. The properties of the epoxy and the nanocomposites during polymerization.

Sample	Silica volume percentage (%)[a]	Relative n increase (%)[b]	Specific refract. ($cm^3\ g^{-1}$)	Relative ρ increase (%)[b]	Interparticle distance (nm)[c]
100 : 14.2 : 0	0	1.6 ± 0.1	0.285 ± 0.005	3.6 ± 0.3	—
100 : 14.2 : 11	5 ± 1	1.5 ± 0.1	0.271 ± 0.005	3.2 ± 0.3	23 ± 3
100 : 14.2 : 25	11 ± 1	1.5 ± 0.1	0.257 ± 0.005	3.4 ± 0.3	14 ± 2
100 : 14.2 : 67	25 ± 1	1.2 ± 0.1	0.232 ± 0.005	3.0 ± 0.3	6 ± 1

[a] Absolute increase during polymerization below 1% .
[b] Determined between 0.8 and 13 h.
[c] Mean interparticle (surface–surface) distance according to Bansal and Ardell [30].

linearly extrapolated refractive indices at $t = 0\,h$, the specific refractivity values indicated in table 3 were obtained. For the pure epoxy, this value is in agreement with published data [28]. The specific refractivity of pure epoxy remains unaltered during polymerization [28]. It is reasonable to assume that the specific refractivity of the silica nanoparticles is not changed during polymerization. In that case, the specific refractivities of the nanocomposites can be net constant. As expected, the mass density of the composites scales with the amount of silica. Between 0.8 and 13 h of polymerization, a relative density increase of 3–3.6% is observed (see table 3), which is consistent with earlier publications [28].

The longitudinal and shear moduli of the pure epoxy and the three nanocomposites were calculated using equation (3). All elastic moduli curves indicated in figure 4 show a nonlinear increase, usually observed during the polymerization of epoxies and polyurethanes at hypersonic frequencies [6, 7, 13, 14]. According to the gCR in figure 5, a gCR is observed for each sample within the margin of error (filled symbols). Astonishingly, even the values of the parameter A (3.1 ± 0.1 GPa) are equal within the margin of error for all nanocomposites, independently of the concentration of silica nanoparticles. This statement is, of course, restricted to the nanoparticle concentrations investigated so far, which on the other hand is rather high.

To avoid any misunderstanding: the existence of a common gCR does not mean that the nanoparticles have no influence on the elastic moduli of the composites. The stiffening effect caused by increasing the amount of nanoparticles on the composites as shown in figure 4 is evidenced in the gCR by a shift of the related $(c_{44}^{\infty}; c_{11}^{\infty})$ data points to higher values. This shift of the elastic moduli data does not affect the Cauchy parameter A for the considered material class. In other words, any morphological features related to the nanoparticles such as particle size, surface corrugation and the formation of mechanical interphases around the particles inside the epoxy matrix, influence the shift of the $(c_{44}^{\infty}; c_{11}^{\infty})$ data on the gCR without violating this relation. Something similar happens around the thermal glass transition of viscous liquids [8]: the gCRs of the liquid and the glassy state are identical, but the $(c_{44}^{\infty}; c_{11}^{\infty})$ data points of the glassy state exceed those of the liquid state. However, for the same temperature changes the elastic data points are distributed denser for the glassy than for the liquid region of the gCR.

The possibility of describing the mechanical properties of the nanocomposites by the same gCR leads to a striking result. Once the Cauchy parameter A of the pure epoxy's gCR has been determined by measuring for instance the longitudinal and shear modulus of the polymerized

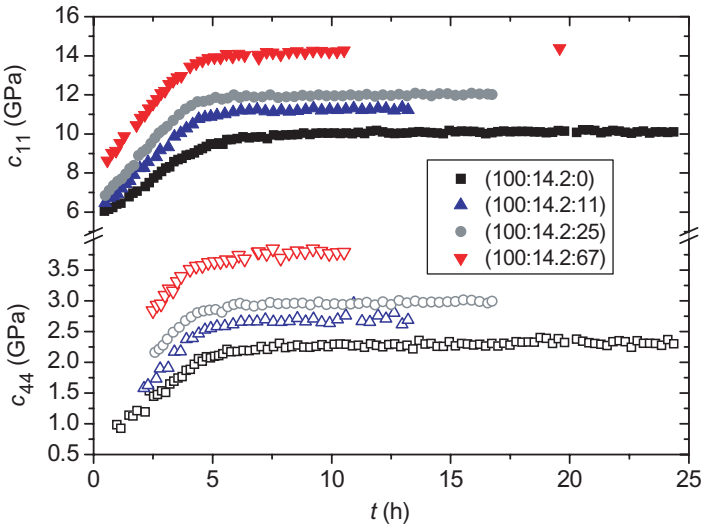

Figure 4. Longitudinal moduli c_{11} (filled symbols) and shear moduli c_{44} (open symbols) versus time during polymerization at 298 K for the epoxy (100 : 14.2 : 0) and the three epoxy/silica nanocomposites.

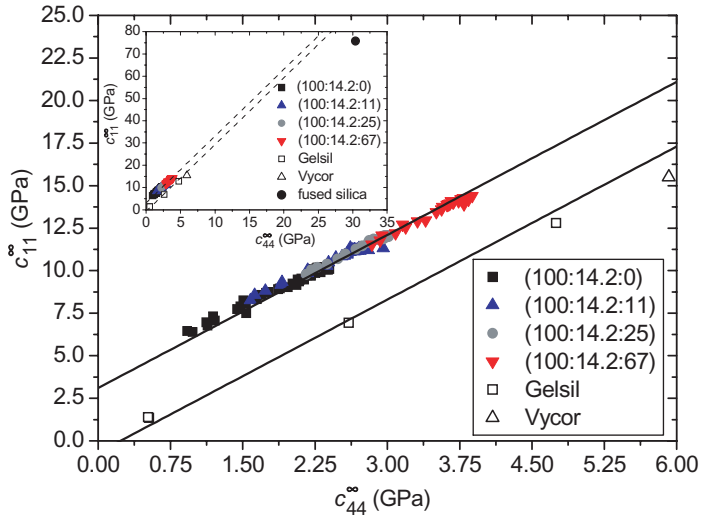

Figure 5. Filled symbols: gCR during the polymerization of the epoxy (100 : 14.2 : 0) and the three nanocomposites. Open symbols: gCR as seen by porous silica glasses with different porosity. Inset: comparison between the aforementioned gCRs and the elastic moduli of fused silica [22] (black dot).

pure epoxy, the shear moduli of the polymerizing nanocomposites can be predicted on the basis of the measured longitudinal moduli. In other words, the Cauchy parameter A of the nanocomposites can be derived from a material, the pure epoxy, which has never been in contact with a silica nanoparticle! The invariance of the Cauchy parameter is even more astonishing if one takes into account that different reactive polyurethane mixtures lead, during polymerization, to gCRs with slightly different Cauchy parameters [14].

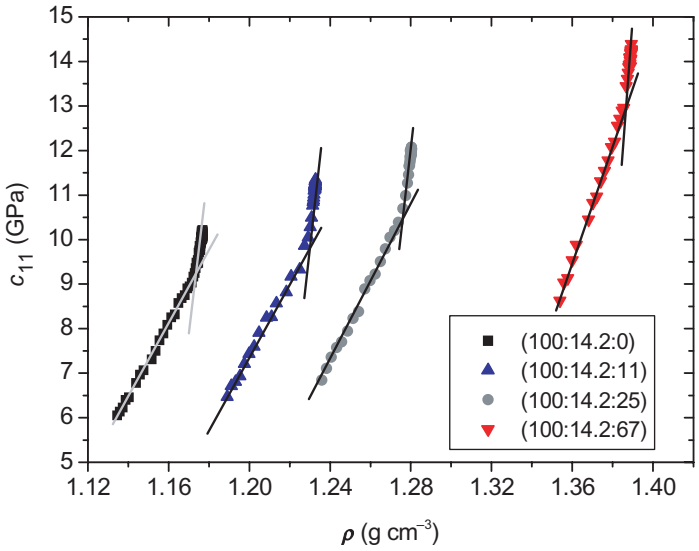

Figure 6. Longitudinal moduli c_{11} versus the density ρ for the pure epoxy and the three nanocomposites during polymerization.

The striking question arises whether the same gCR observed for all epoxy/silica nanocomposites can be maintained until much higher silica concentrations, which means until a state when the silica nanoparticles are percolated. Such a state could be approximated by a nanoporous silica glass, where pores are filled with epoxy. Unfortunately, we have not yet been able to fill the pores of the silica glasses mentioned in table 2 with epoxy. However, the longitudinal and shear moduli of these porous glasses filled with air could be studied by BS and are indicated in table 2. The gCR related to the increasing porosity (respectively the decreasing density) of the glasses is shown in figure 5 (open symbols). Only the Gelsil glasses were used for the fit, as the Vycor and Gelsil glasses are produced by different processes and possess an unknown contamination of the pore walls (at least moisture). The freely fitted slope equals 2.7, which is within the margin of error compatible with 3. The Cauchy parameter A determined as a function of the Gelsil glasses' porosity corresponds to -0.7 ± 0.4 GPa when the gCR's slope is fixed at 3. It is worth noting that the elastic properties of the Vycor glass fit well to those of the Gelsil glasses in the gCR representation. In contrast with the epoxy/silica nanocomposites, the silica matrices of the porous glasses are percolated and the pores are predominantly filled with air instead of epoxy. In the inset of figure 5 the elastic moduli of the inorganic fused silica glass [22] (black dot) are compared with those of the nanocomposites and the porous glasses. Obviously, the porous silica glasses' absolute values of the elastic moduli are much closer to those of the silica-filled epoxies (organic glasses) than to those of the inorganic fused silica glass. In addition, the fused silica data point deviates significantly from the indicated gCRs. The 'small' difference between the Cauchy parameters A of the nanocomposites and the porous glasses is astonishing.

As observed for all the epoxies and polyurethanes investigated so far [6, 7, 9, 10, 13, 14], the isostructural chemically induced sol–gel and glass transitions of the nanocomposites are hidden in the gCR. Figure 6 shows an alternative representation: the longitudinal modulus versus the density during polymerization. Within the margin of error, these curves increase linearly at the beginning of polymerization and show a strong bending

upwards above material-specific densities ρ_s. These material-specific densities are likely to be indicative of the onset of the chemically induced sol–gel and/or glass transition, when considering a similar behavior reported at the thermal glass transition of structural glasses [31]. The change in the linear relation between elastic moduli and density is indicative either of a change in the anharmonic part of the mechanical interaction potential or of morphological changes around ρ_s. Since we observe only one slope change in the $c_{11}(\rho)$-representation and since we cannot discriminate, from our data, between morphological changes and anharmonicity, we are not able to relate the $c_{11}(\rho)$-anomaly to either gelation or vitrification. It is even possible that both transformations are temporally so close to each other that the observed anomaly reflects both. The linearity of the nanocomposites' gCRs shows that these mechanical anomalies are not reflected by this representation. Obviously, the linearity of the gCR is also not broken by the non-equilibrium process of polymerization. This is interpreted as a hint to a local equilibrium achieved by the longitudinal and shear moduli in the course of the rather slow polymerization process [14]. Whether the observed gCRs are still valid if the polymerization process is significantly accelerated is a topic of further study.

5. Conclusion

Astonishingly, epoxy/silica nanocomposites with varied filler content follow the same gCR as the pure epoxy during polymerization. Even the chemically induced sol–gel and glass transitions are hidden. The identical Cauchy parameter A for the studied silica concentrations implies that once the value of this Cauchy parameter has been determined, the shear moduli of the polymerizing nanocomposites can be estimated on the basis of the measured longitudinal moduli c_{11}. The specific properties of the silica nanoparticles and their distribution within the composites influence the location of the $(c_{44}^{\infty}; c_{11}^{\infty})$ data points on the gCR rather than violate this representation. Surprisingly, porous silica glasses show, as a function of porosity, a gCR similar to that of the epoxy/silica nanocomposites. Optically relevant interphases are not observed. Mechanically relevant interphases could also not be detected in the nanocomposites when considering the gCR. The apparent insensitivity of the generalized Cauchy representation to mechanical interphases can be understood if these additional 'phases' act on the longitudinal and shear modulus according to a linear transformation. In contrast with this representation, the $c_{11}(\rho)$-representation is sensitive to the chemically induced sol–gel and/or glass transition but these transitions cannot be distinguished yet.

Acknowledgments

This work was financially supported by the project 'Static and Dynamic Properties of Nanocomposites' (University of Luxembourg) and the Ministère de la Culture, de l'Enseignement Supérieur et de la Recherche du Grand-Duché du Luxembourg. We thank Dr A le Coutre for some of the measurements on porous glasses.

References

[1] Auld B A 1973 *Acoustic Fields and Waves in Solids,* vol 1 (New York: Wiley)
[2] Nye J F 1972 *Physical Properties of Crystals* (Oxford: Oxford University Press)

[3] Sommerfeld A 1945 *Vorlesungen über theoretische Physik, Band 2, Mechanik der deformierbaren Medien* (Leipzig: Harri Deutsch)
[4] Grimvall G 1986 *Thermophysical Properties of Materials* (Amsterdam: North-Holland)
[5] Ward I M 1971 *Mechanical Properties of Solid Polymers* (London: Wiley)
[6] Yamura H, Matsukawa M, Otani T and Ohtori N 1999 *Japan J. Appl. Phys.* **38** 3175–8
[7] Krüger J K, Baller J, Britz T, le Coutre A, Peter R, Bactavatchalou R and Schreiber J 2002 *Phys. Rev.* B **66** 012206
[8] Krüger J K, Britz T, le Coutre A, Baller J, Possart W, Alnot P and Sanctuary R 2003 *New J. Phys.* **5** 80
[9] Krüger J K *et al* 2005 *J. Physique IV* **129** 45–9
[10] Bactavatchalou R 2006 *J. Phys.: Conf. Ser.* **40** 111
[11] Wen P, Johari G P, Wang R J and Wang W H 2006 *Phys. Rev.* B **73** 224203
[12] Pineda E and Crespo D 2008 *Rev. Adv. Mater. Sci.* **18** 173–6
[13] Fioretto D, Corezzi S, Caponi S, Scarponi F, Monaco G, Fontana A and Palmieri L 2008 *J Chem. Phys.* **128** 214502
[14] Philipp M, Vergnat C, Müller U, Sanctuary R, Baller J, Possart W, Alnot P and Krüger J K 2009 *J. Phys.: Condens. Matter* **21** 035106
[15] Wetzel B, Rosso P, Haupert F and Friedrich K 2006 *Eng. Fract. Mech.* **73** 2375–98
[16] Possart W 2005 *Adhesion, Current Research and Applications* (Weinheim: Wiley)
[17] Philipp M, Gervais P C, Sanctuary R, Müller U, Baller J, Wetzel B and Krüger J K 2008 *Express Polym. Lett.* **2** 546–52
[18] de Gennes P G 1979 *Scaling Concepts in Polymer Physics* (Ithaca, NY: Cornell University Press)
[19] Brinker C J and Scherer G W 1990 *Sol–Gel Science—The Physics and Chemistry of Sol–Gel Processing* (New York: Academic)
[20] Donth E 1992 *Relaxation and Thermodynamics in Polymers, Glass Transition* (Berlin: Akademie-Verlag)
[21] Krüger J K 2007 *Ageing and the Glass Transition* (*Lecture Notes in Physics* vol 716) ed M Henkel, M Pleimling and R Sanctuary (Berlin: Springer)
[22] Le Parc R, Levelut C, Pelous J, Martinez V and Champagnon B 2006 *J. Phys.: Condens. Matter* **18** 7507–27
[23] Johnson B B, Kinloch A J, Mohammed R D, Taylor A C and Sprenger S 2007 *Polymer* **48** 530–41
[24] Kinloch A J, Mohammed R D, Taylor A C, Eger C, Sprenger S and Egan D 2005 *J. Mater. Sci.* **40** 5083–6
[25] Blackman B R K, Kinloch A J, Sohn Lee J, Taylor A C, Agarwal R, Schueneman G and Sprenger S 2007 *J. Mater. Sci.* **42** 7049–51
[26] Kinloch A J, Lee J H, Taylor A C, Sprenger S, Eger C and Egan D 2003 *J. Adhes.* **79** 867–73
[27] Rosso P and Ye L 2007 *Macromol. Rapid Commun.* **28** 121–6
[28] Wehlack C, Possart W, Krüger J K and Müller U 2007 *Soft Mater.* **5** 87–134
[29] Baller J 2009 in review
[30] Bansal P P and Ardell A J 1972 *Metallography* **5** 97–111
[31] Krüger J K 1989 *Optical Techniques to Characterize Polymer Systems* ed H Bässler (Amsterdam: Elsevier)
[32] Lorentz H A 1880 *Wied. Ann. Phys.* **9** 641
[33] Lorenz L V 1880 *Wied. Ann. Phys.* **11** 70
[34] Zwanzig R and Mountain R D 1965 *J. Chem. Phys.* **43** 4464
[35] Born M and Wolf E 1999 *Principles of Optics* (Cambridge: Cambridge University Press)
[36] Morse P M and Uno Ingard K 1968 *Theoretical Acoustics* (Princeton, NJ: Princeton University Press)